Manchester Metropolitan University

e-space

Manchester Metropolitan University's Research Repository

Please cite the Published Version

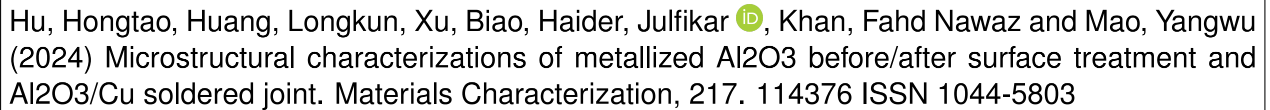

Hu, Hongtao, Huang, Longkun, Xu, Biao, Haider, Julfikar, Khan, Fahd Nawaz and Mao, Yangwu (2024) Microstructural characterizations of metallized Al2O3 before/after surface treatment and Al2O3/Cu soldered joint. Materials Characterization, 217. 114376 ISSN 1044-5803

DOI: https://doi.org/10.1016/j.matchar.2024.114376

Publisher: Elsevier

Version: Accepted Version

Downloaded from: https://e-space.mmu.ac.uk/635528/

Usage rights: Creative Commons: Attribution 4.0

Additional Information: This is an accepted manuscript of an article which appeared in final form in Materials Characterization

Data Access Statement: The data that has been used is confidential.

Enquiries:
If you have questions about this document, contact openresearch@mmu.ac.uk. Please include the URL of the record in e-space. If you believe that your, or a third party's rights have been compromised through this document please see our Take Down policy (available from https://www.mmu.ac.uk/library/using-the-library/policies-and-guidelines)

Low-temperature joining of metallized Al_2O_3 ceramics to Cu

Hongtao Hu [a], Longkun Huang [a], Biao Xu [a], Julfikar Haider [b], Fahd Nawaz Khan [c], Yangwu Mao [a,d,*]

[a] Hubei Key Laboratory of Plasma Chemistry and Advanced Materials, Wuhan Institute of Technology, Wuhan 430205, China

[b] Department of Engineering, Manchester Metropolitan University, Manchester M1 5GD, UK

[c] Faculty of Materials and Chemical Engineering, Department of Materials Science, Ghulam Ishaq Khan Institute of Engineering Sciences and Technology, Topi 23640, Pakistan

[d] Key Laboratory of Green Chemical Engineering Process of Ministry of Education, Wuhan Institute of Technology, Wuhan 430205, China

* Corresponding author, Email: myw@wit.edu.cn

Tel: +86-27-87195661

Fax: +86-27-87195661

Abstract: Joining Al_2O_3 ceramics to Cu heat pipes should be conducted at low temperatures since Cu heat pipes may fail at the temperatures higher than 320°C. Due to the poor wettability of low-temperature solder on Al_2O_3 ceramics, it is essential to metallize the Al_2O_3 ceramics before joining Al_2O_3 to Cu with a low-temperature solder. Surface metallization of Al_2O_3 has been conducted using Ag-Cu-Ti active metal filler at 900°C. Microanalysis indicates that the interfacial reaction occurs between the active metal filler and the Al_2O_3, leading to the formation of a Cu_3Ti_3O reaction layer. The metal layer on the surface of Al_2O_3 is primarily composed of Ag ss (solid solution), Cu ss and

Ti_2Cu. The polishing treatment of the surface metal layer in the metallized Al_2O_3 results in a reduction of the oxide content and contaminants, which contributes to the subsequent low-temperature joining. Low-temperature joining of the metallized Al_2O_3 to Cu has been carried out using Sn-Ag-Cu solder at 280°C. The joining area of the joint includes a Cu_3Ti_3O reaction layer, a metal layer and a solder layer. The solder layer mainly consists of Sn ss, Ag_3Sn and Cu_6Sn_5. The Al_2O_3/Cu joint fractures in the solder layer after shearing test, indicating that the strength of the solder is relatively low. However, the interfacial bonding between the metallized Al_2O_3, the solder layer and the Cu base material is satisfactory.

Keywords: A. Al_2O_3 ceramics; B. Metallization; C. Low temperature joining; D. microstructure

1. Introduction

Joining of Al_2O_3 ceramics to Cu heat pipes is a fundamental aspect of the heat dissipation of high-power devices in electronic applications [1]. Brazing is an effective technique for joining Al_2O_3/Cu due to its relatively simple processing, low cost and high reliability [2-10]. Yuan et al. [7] employed a brazing technique using Cu-Sn-Ti filler at a temperature of 930°C to join Al_2O_3 to Cu. The results demonstrated that the joining layer of the joint mainly comprised of TiO, Cu_3Ti_3O and Cu-Ti intermetallics. Fan et al. [8] employed a brazing technique utilizing Ag-Cu-Ti + Zn composite filler at a temperature of 900°C for the joining of Al_2O_3 to Cu. The findings demonstrated that the tensile strength of the joint

with composite filler was enhanced to 20.89 MPa, representing an increase of 67.6% in comparison to the joint without the Zn foil. Jin et al. [9] conducted a study on Al_2O_3/Cu brazing with Ag-Cu-Ti +W composite filler. The shear strength of the joint with composite filler was observed to increase to 32.7 MPa, in comparison to that without the W foil (24.9 MPa). Furthermore, Fu et al. [10] metallized Al_2O_3 by utilizing Sn-0.3Ag-0.7Cu-6Ti metal powder at 900°C, after which the metallized Al_2O_3 was brazed to Cu using Sn-0.3Ag-0.7Cu filler at 580°C ~660°C for 5 minutes. The highest joint shear strength was found to be 32 MPa when brazing was conducted at 620°C.

Given that Cu heat pipes may undergo expansion and deformation with an increase in temperature, potentially leading to failure at 320°C [11], brazing of Al_2O_3 ceramics to Cu heat pipes is not a suitable approach. This is because the brazing temperature typically exceeds 500°C. Consequently, joining of Al_2O_3 ceramics to Cu heat pipes must be conducted at a low temperature. In view of the poor wettability of the low-temperature solder on the Al_2O_3 ceramics, it is recommended that surface metallization of the Al_2O_3 ceramics be carried out prior to joining the Al_2O_3 to Cu at low temperatures with a solder.

In this study, surface metallization of Al_2O_3 ceramics was conducted using an active Ag-Cu-Ti braze. In order to investigate the effect of surface treatment on the low-temperature joining of metallized Al_2O_3 ceramics to Cu, the microstructure and element distribution of the as-received and polished metal layer in the metallized Al_2O_3 ceramics were characterized. Subsequently, the metallized Al_2O_3 was joined to Cu using Sn-Ag-Cu solder at a low temperature. The joint microstructure and mechanical properties were

explored.

2. Experimental

2.1 Materials

The Al_2O_3 substrates, with a purity of 95.0 %, a density of 3.60 g/cm^3 and a size of 10× 10 × 6 mm^3, were procured from Shanghai Xinmao Precision Ceramics Technology Co., Ltd., China. The Cu substrates, with a purity of 99.9 %, a density of 8.90 g/cm^3 and a size of 10 × 10× 10 mm^3, were provided by Beijing Tiancheng Jida Metal Co., Ltd., China. The Ag-Cu-Ti (Ag: 68.8 wt.%, Cu: 26.7 wt.%, Ti: 4.5 wt.%) paste? used for the surface metallization of Al_2O_3 ceramics was procured from Changsha Tianjiu Metal Materials Co., Ltd., China. The melting temperature of the Ag-Cu-Ti braze was found to be between 770°C and 810°C, while the metallization temperature was set at 900°C. The Sn-Ag-Cu (Sn: 96.5 wt.%, Ag: 3.0 wt.%, Cu: 0.5 wt.%) solder used for low-temperature joining of the metallized Al_2O_3 ceramics to Cu was purchased from Zhenjiang Pan-Ada Electronic Technology Co., Ltd., China. The melting temperature of the Sn-Ag-Cu solder was 217°C. The as-received Al_2O_3 and Cu substrates were polished with SiC sandpaper in order to remove any impurities or contaminants. Subsequently, the polished samples were subjected to ultrasonic cleaning in deionized water and in ethanol for 15 minutes each.

2.2 Surface metallization of Al_2O_3

The surface metallization of Al_2O_3 was conducted with Ag-Cu-Ti filler under vacuum

conditions. The Ag-Cu-Ti paste was applied to the surface of the Al_2O_3 to be joined (as illustrated in **Fig. 1a**), and subsequently, the Al_2O_3 coated with the paste was transferred into a molybdenum wire furnace. The coated Al_2O_3 samples were heated from room temperature to 500°C at a heating rate of 10°C/min, and maintained at 500°C for 30 minutes to evaporate the organic solvent in the paste. The temperature was then increased to 750°C at a rate of 10°C/min and subsequently to 900°C at a rate of 5°C/min. Following the surface metallization at 900°C for 10 minutes, the samples were cooled from 900°C to 600°C at a cooling rate of 5°C/min and then to room temperature via furnace cooling.

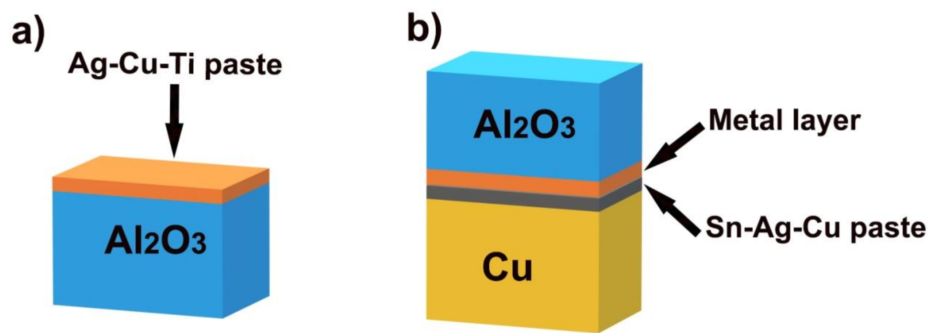

Fig. 1. Schematic of surface metallization of Al_2O_3 with Ag-Cu-Ti paste a) and low temperature joining of metallized Al_2O_3 to Cu with Sn-Ag-Cu solder b).

2.3 Low-temperature joining process

The metal layer in the metallized Al_2O_3 ceramics was polished with 300 # SiC sandpaper to remove an oxide layer of approximately 15 µm. Low-temperature joining of the metallized Al_2O_3 ceramics to Cu was carried out using Sn-Ag-Cu solder. The Sn-Ag-Cu solder was applied to the surface of the Cu substrate that was to be joined, and then the Cu coated with solder was assembled with the metallized Al_2O_3 to form a sandwich

structure (as illustrated in **Fig. 1b**). Subsequently, the assembled joining couple was placed on a hot plate. Given the excellent thermal conductivity of Cu, direct contact between the Cu substrate and the hot plate was permitted. In addition, in order to facilitate interfacial bonding between the solder and the substrates, a pressure of 4.7 kPa was applied to the assembly. The low-temperature joining process was conducted at 280°C for a period of 90 seconds.

2.4 Microstructural and mechanical characterizations

The morphology of the metal layer and interfacial region in the metallized Al_2O_3, the interfacial region in the Al_2O_3/Cu joint and the fracture of the joint after shearing tests were observed using GeminiSEM 300 Field Emission Scanning Electron Microscopy (FESEM). The corresponding element compositions were characterized using the attached Oxford Inca X-Act Energy Dispersive Spectroscopy (EDS). The Bruker D8 Advance X-ray Diffraction (XRD) instrument was employed to ascertain the phases present in the metal layer of the metallized Al_2O_3 and in the interfacial region of the Al_2O_3/Cu joint. The acceleration voltage was set at 40 kV, the wavelength of the Cu target k_α was 0.15418 nm, the scanning range was 10°~90°, and the scanning speed was 4°/min. Escalab 250Xi X-ray photoelectron spectroscopy (XPS) was employed to analyze the elemental composition of the metal layer in the metallized Al_2O_3.

The HXD-1000TMC/LCD Vickers hardness indenter was employed to ascertain the microhardness values of the Al_2O_3/Cu joint. Given the considerable variation in hardness

observed across the different components of the joint, the load applied during hardness testing was set at 9.8 N for the Al_2O_3 substrate, 0.98 N for the metal layer and Cu substrate, and 0.098 N for the solder layer. At least three analogous locations were evaluated to ascertain the mean microhardness. The shear strength of the joints was determined using the GP-TS2000s electronic universal testing machine, with a loading speed of 0.5 mm/min. At least three joints produced by the same joining parameters were measured in order to calculate the average shear strength.

3. Results and Discussion

3.1 Surface metallization of Al_2O_3 using Ag-Cu-Ti filler

Fig. 2 illustrates the micro-morphology and elemental distributions of the interfacial region in the metallized Al_2O_3 using Ag-Cu-Ti filler. As shown in **Fig. 2a**), favorable interfacial bonding is achieved between the Al_2O_3 and the metal layer. The elemental distributions depicted in **Fig. 2b-f**) reveals that the metal layer primarily comprises of Ag, Cu and Ti. The distribution of Ag is concentrated in the light grey region of the metal layer, while Cu and Ti are predominantly present in the grey region. In addition, it can be seen in **Fig. 2f**) that Ti enrichment occurs at the Al_2O_3/metal layer interface (approximately 2~5 μm thick), indicating that a reaction region has been formed due to the interfacial reaction of Ti in the filler with Al_2O_3 substrate. Ali et al. [12] also observed the formation of a reactive region with a thickness of about 3~6 μm at the Al_2O_3 /brazing layer interface during Al_2O_3/Al_2O_3 brazing with Ag-Cu-Ti filler.

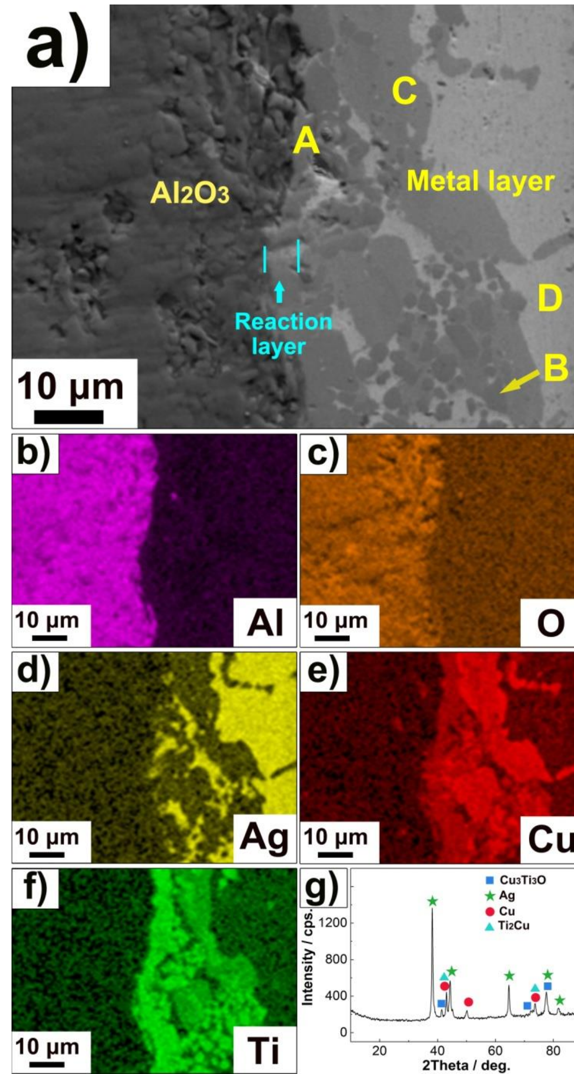

Fig. 2. Micro-morphology a), elemental distributions b-f) and XRD pattern g) of the interfacial region in the metallized Al_2O_3 using Ag-Cu-Ti filler.

Table 1 presents the EDS results of the microregions marked in Fig. 2a). The microregion A, situated within the reaction layer, is primarily composed of elements Cu, Ti and O, which can be inferred as Cu_3Ti_3O. In a previous study, Li et al. [13] identified the Cu_3Ti_3O reaction region at the Al_2O_3/filler layer interface for the Al_2O_3/304 stainless steel joint brazed using Ag-Cu-Ti + BN composite filler. With regard to the grey

microregion B situated within the metal layer, the atomic ratio of Cu:Ti is found to be approximately 1:2, which correlates well with the formation of Ti_2Cu intermetallics. The grey microregion C in the metal layer contains 70.21 at.% Cu and 27.34 at.% Ti, which is presumed to be a mixture of a Cu ss (solid solution) and Ti-Cu intermetallics. The Ag content in the light grey microregion D of the metal layer is markedly elevated (90.32 at.%), indicative of an Ag ss. The XRD pattern of the metal layer in the metalized Al_2O_3, as shown in Fig. 2g), corroborates the presence of Cu_3Ti_3O, Ag, Cu and Ti_2Cu, in accordance with the EDS findings. In a separate study, Wen et al. [14] proposed that the formation of Ag ss, Cu ss, Ti-Cu intermetallics and Cu_3Ti_3O phase occurred in the brazing area for the Al_2O_3/Cu joint utilizing Ag-Cu-Ti filler.

Table 1. EDS results of microregions in **Fig. 2a**).

Microregions	Compositions (at.%)					Possible phases
	Ag	Cu	Ti	O	Al	
A	1.87	24.78	35.16	33.88	4.31	Cu_3Ti_3O
B	1.77	35.05	63.18	-	-	Ti_2Cu
C	2.45	70.21	27.34	-	-	Cu ss, Ti-Cu
D	90.32	9.53	0.15	-	-	Ag ss

3.2 Surface treatment of the metallized Al_2O_3

Low temperature joining of the metallized Al_2O_3 to Cu has been carried out through the utilization of Sn-Ag-Cu solder. Nevertheless, the joint strength is rather low(may be give

the approximate value), which may be attributed to the presence of an oxide layer on the surface of the metal layer in the metallized Al_2O_3. The oxide layer may impede the wetting and spreading of the liquid solder on the metallized Al_2O_3, resulting in an unsatisfactory interfacial bonding between the metal layer in the metallized Al_2O_3 and the liquid solder. Following the removal of a layer of about 15 μm from the metal layer in the metallized Al_2O_3, low-temperature joining of the metallized Al_2O_3 to Cu was achieved using Sn-Ag-Cu solder at 280°C. This suggests that the removal of the oxide layer in the metallized Al_2O_3 may facilitate low-temperature joining of the metallized Al_2O_3 to Cu. In order to elucidate the elemental composition and chemical state of the metal layer, the as-received and polished surface of the metal layers in the metallized Al_2O_3 have been subjected to characterization.

Fig. 3 shows the morphology and elemental distributions of the as-received surface of the metal layer in the metallized Al_2O_3. As illustrated in **Fig. 3a**), the as-received surface of the metal layer is observed to exhibit a relatively uniform and even appearance. The elemental distributions depicted in **Fig. 3b-e**) reveal that the as-received surface of the metal layer predominantly contains Ag, Cu, Ti and O.

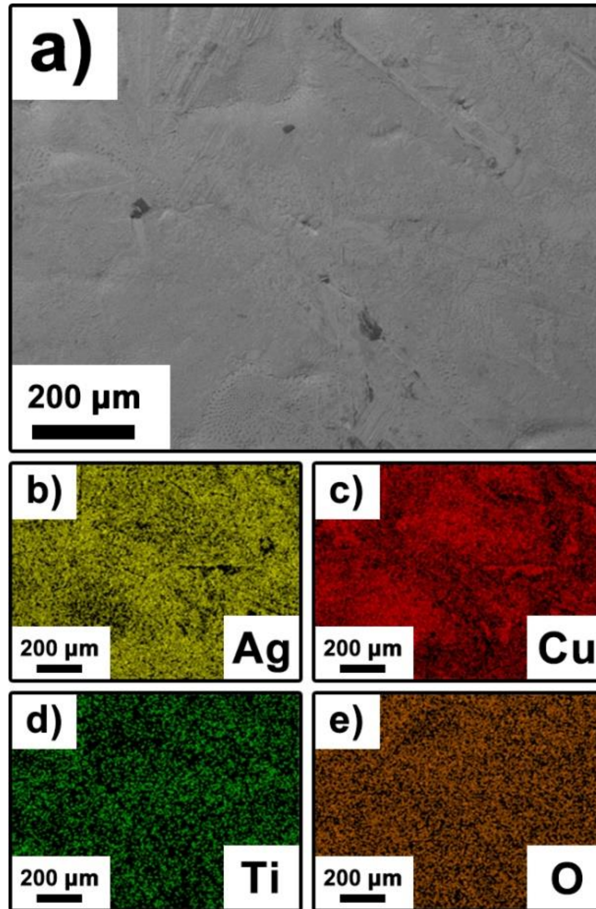

Fig. 3. Morphology a) and elemental distributions b) of the as-received surface of the metal layer in the metalized Al_2O_3.(may be revisit the figure numbers)

The elemental compositions displayed in **Table 2** demonstrate that the as-received surface of the metal layer contains 43.02 at.% O. This substantiates the hypothesis that the metal layer in the metallized Al_2O_3 undergoes substantial oxidation in air, which may lead to inadequate wetting of the solder on the surface of the metal layer, and consequently result in a diminished joining strength of the Al_2O_3/Cu joint.

Table 2. Elemental compositions of the as-received and polished surface of the metal

layer in the metallized Al_2O_3.

Element	As-received surface (at.%)	Polished surface (at.%)
Ag	24.24	54.19
Cu	25.74	35.55
Ti	7.00	1.98
O	43.02	8.28

Fig. 4 shows the morphology and elemental distributions of the polished surface of the metal layer (removal of a layer of approximately 15 μm) in the metallized Al_2O_3. As can be observed in **Fig. 4a**), the polished surface of the metal layer displays a regular pattern of scratches. The presence of these scratches can facilitate increased contact between the metal layer and the solder, which may enhance interfacial bonding in Al_2O_3/Cu soldering.

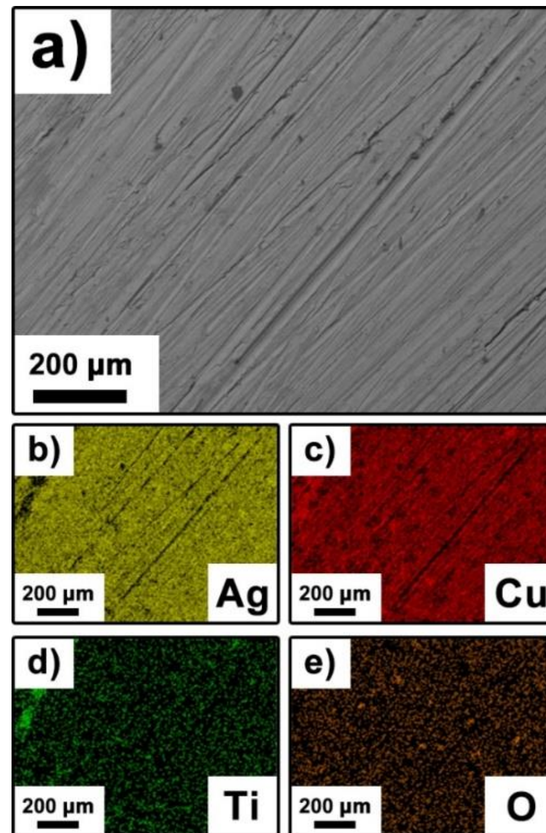

Fig. 4. Morphology a) and elemental distributions b-e) of the polished surface of the metal layer (removal of about 15 μm) in the metallized Al_2O_3.

The elemental distributions depicted in **Fig. 4b-e**) reveal that the polished surface of the metal layer in the metallized Al_2O_3 mainly comprises of Ag, Cu, Ti and O, exhibiting a similar composition to that observed in the as-received surface of the metal layer. However, the oxygen content in the polished surface of the metal layer (**Table 2**) is significantly reduced, reaching 8.28 at.% (in comparison, the oxygen content in the as-received surface is 43.02 at.%). This suggests that the majority of the surface oxide in the metal layer can be removed through polishing, which is advantageous for the wetting of the liquid solder on the metallized Al_2O_3.

Fig. 5 displays the XPS spectra of the as-received surface of the metal layer in the metallized Al_2O_3. As illustrated in **Fig. 5a**), the as-received surface of the metal layer exhibits the presence of Ag, Cu, Ti, O and C. It is noteworthy that the peak intensities of Ag, Cu and Ti are comparatively weaker than those of C and O. This may be caused by the presence of adsorbed O_2, H_2O and hydrocarbon compounds in the surrounding environment. Similarly, Saleh et al. [15] observed high peak intensities of C and O in XPS patterns, which they attributed to exposure to air when studying the oxidation mechanism of Mg alloy using XPS.

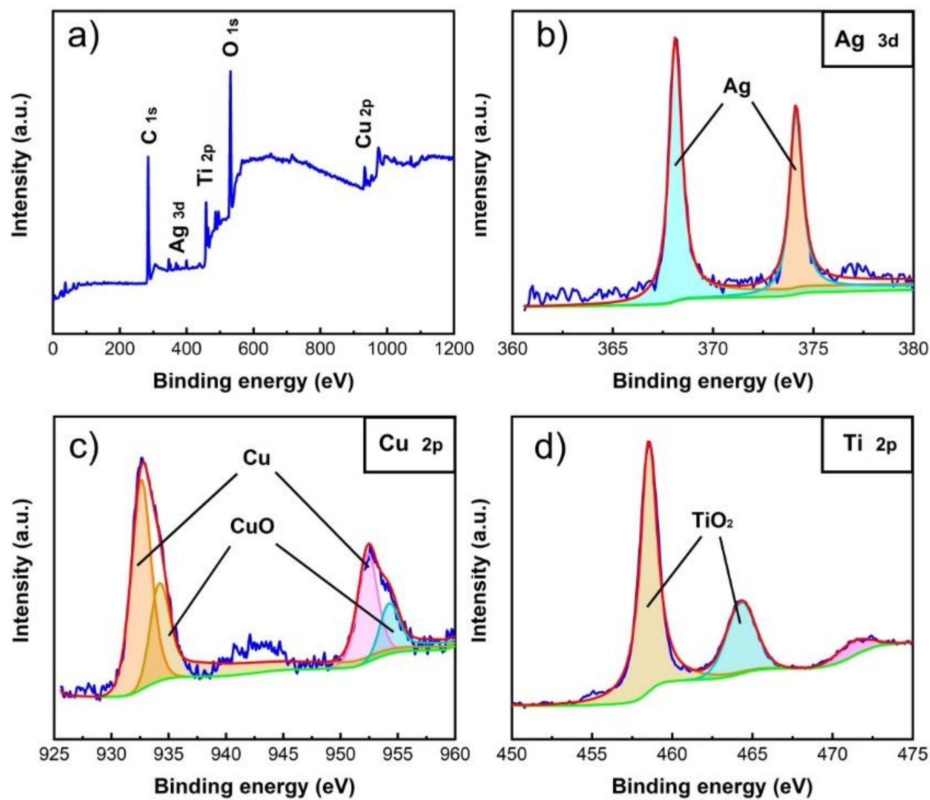

Fig. 5. XPS spectra of the as-received surface of the metal layer in the metallized Al_2O_3. a) full XPS spectrum, b) Ag 3d, c) Cu 2p and d) Ti 2p.

The XPS result of Ag 3d (**Fig. 5b**) indicates that the double peaks at binding energies of 368.2 eV and 374.2 eV correspond to Ag [16]. This suggests that no oxidation of the Ag occurs on the surface of the as-received metal layer. Graedel [17] asserted that Ag exhibited enhanced oxidation resistance in air at low temperatures. The XPS result of Cu 2p (**Fig. 5c**) demonstrates the existence of Cu (corresponding to the binding energies of 932.5 eV and 952.1 eV) and CuO (corresponding to the binding energies of 934.0 eV and 954.0 eV) in the as-received surface of the metal layer [18,19]. The XPS result of Ti 2p (**Fig. 5d**) indicates the formation of TiO_2 (corresponding to the binding energies of 458.3 eV and 464.1 eV) [20,21]. Ma et al. [22] proposed that a thin oxide layer was formed at room temperature when investigating the surface oxidation mechanism of Ti alloy.

Fig. 6 illustrates the XPS spectra of the polished surface of the metal layer in the metallized Al_2O_3. The full spectrum (**Fig. 6a**) reveals that the polished surface still contains Ag, Cu, Ti, O, and C. However, in comparison to the XPS result of the as-received metal layer, the peak intensities of O and C exhibit a notable decrease, while the peak intensities of Ag and Cu demonstrate a significant increase. This suggests that most of the oxides and contaminants on the surface of the metal layer have been removed after polishing, which may prove advantageous for the subsequent low-temperature joining of the metallized Al_2O_3 to Cu.

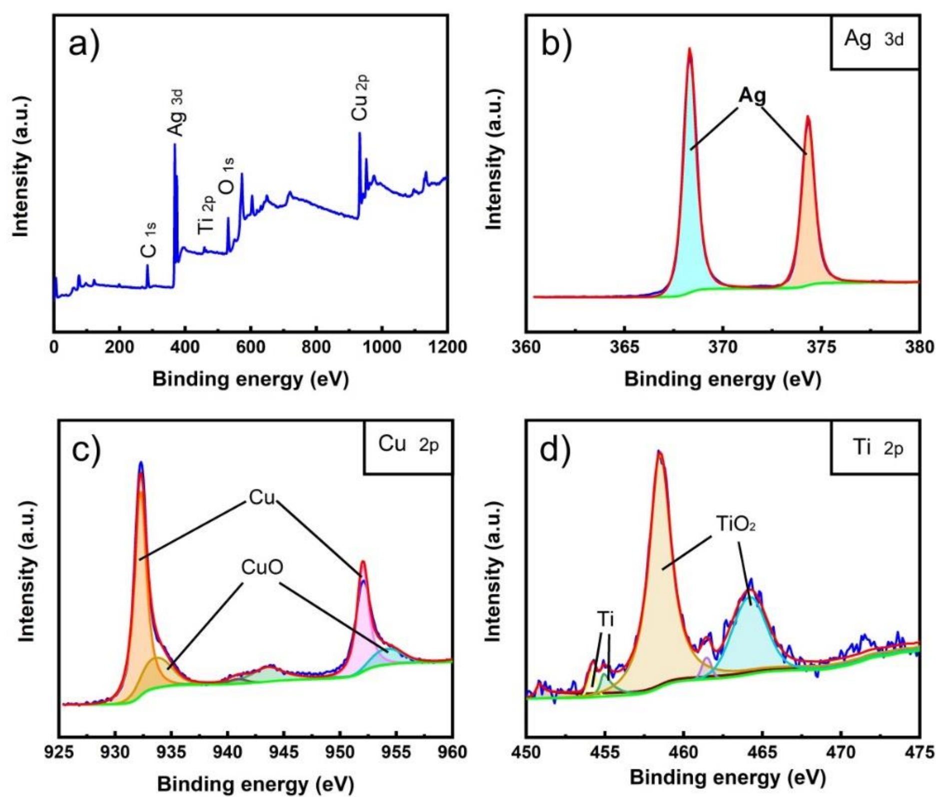

Fig. 6. XPS spectra of the polished surface of the metal layer in the metallized Al_2O_3.

a) full XPS spectrum, b) Ag 3d, c) Cu 2p and d) Ti 2p.

The XPS pattern of Ag 3d (**Fig. 6b**) confirms non-oxidation of Ag in the metal layer. The XPS result of Cu 2p (**Fig. 6c**) indicates that the characteristic peak intensities of Cu (binding energies of 932.5 eV and 952.1 eV) are significantly higher than those of CuO. This suggests a high content of Cu and a small amount of CuO in the polished surface of the metal layer. A comparison of the XPS patterns of Cu 2p on the as-received surface of the metal layer with those of the polished surface reveals a significant reduction in peak intensities for CuO, indicating that the majority of this compound can be removed by polishing. In addition, the XPS result of Ti 2p (**Fig. 6d**) indicates the presence of TiO_2

and trace Ti, which suggests that Ti is highly susceptible to oxidation.

The XPS results of the as-received and polished surface of the metal layer in the metallized Al_2O_3 indicate the presence of a high content of CuO and the adsorption of C-H and oxygen in the as-received metal layer. This may result in the unsatisfactory interfacial bonding of the Sn-Ag-Cu solder with the metallized Al_2O_3 in low-temperature joining, thereby leading to a low joining strength of joint. The polishing of the metal layer may contribute to the formation of a larger contact area between the liquid solder and the metal layer, as well as the reduction of oxide and contaminants, which are beneficial for the subsequent low-temperature joining of the metallized Al_2O_3 to Cu. It is important to note that TiO_2 still exists on the polished surface of the metal layer. As the Ti content in the Ag-Cu-Ti filler is relatively low (4.5 wt.%) and most of the Ti is involved in the reaction with Al_2O_3, the residual TiO_2 is unlikely to have a significant effect on the low-temperature joining process.

3.3 Microstructure of Al_2O_3 /Cu joint

Fig. 7 shows the microscopic morphology and elemental distributions of the Al_2O_3/Cu joint using Sn-Ag-Cu solder. As displayed in **Fig. 7a**), the interfacial bonding between the Al_2O_3, the metal layer, the solder layer and the Cu base material is deemed to be satisfactory. The metal layer and the solder layer exhibit thicknesses of about 37 μm and 180 μm, respectively.

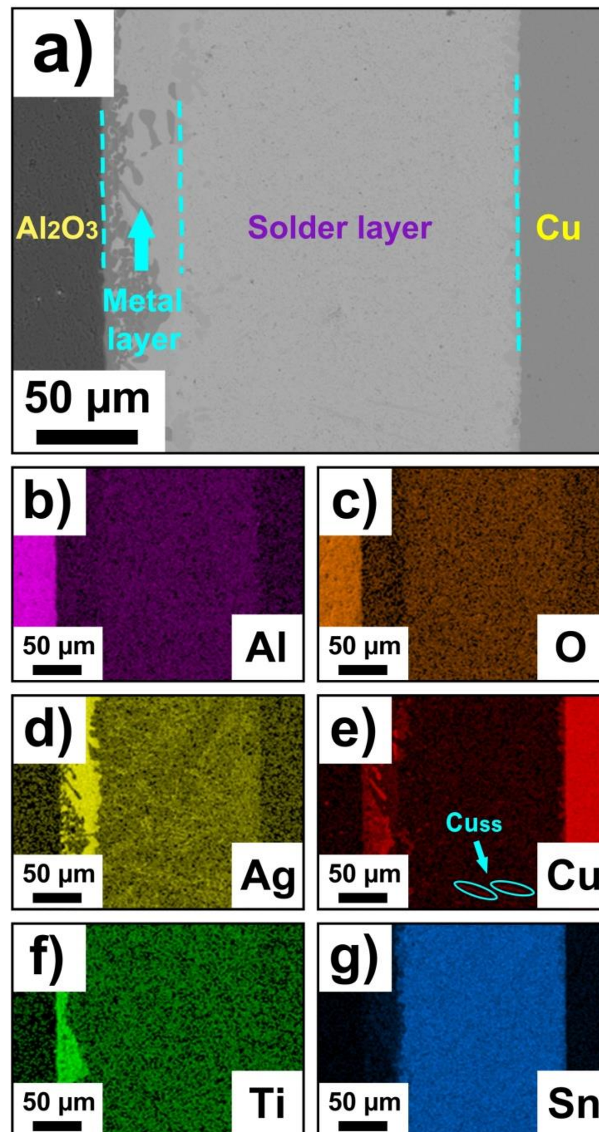

Fig. 7. Micro-morphology a) and elemental distributions b-g) of the Al_2O_3/Cu joint using Sn-Ag-Cu solder.

A comparison of the elemental distributions in Fig. 7b-g) reveals that the metal layer contains Ag, Cu and Ti, whereas the solder layer contains Sn, Ag and Cu. The distributions of the elements in both the metal layer and solder layer are consistent with the compositions of the Ag-Cu-Ti filler and the Sn-Ag-Cu solder. Notably, the solder layer

displays a clear Cu enrichment, as indicated by the circles marked in **Fig. 7e**). Taking into account the low content of Cu (0.5 wt.%) in the Sn-Ag-Cu solder, it can be postulated that the Cu enrichment in the solder layer is a consequence of the dissolution and diffusion of the Cu base material. Izuta et al. [23] asserted that the Cu base material could dissolve into the liquid Sn-Ag-Cu solder at temperatures between 230°C and 300°C during the soldering process.

Fig. 8 presents an enlarged view of the interfacial region in the Al_2O_3/Cu joint. The element compositions of the microregions depicted in **Fig. 8** are presented in **Table 3**. The microregion A in the reaction region close to the Al_2O_3 side mainly contains Cu, Ti and O, which is indicative of Cu_3Ti_3O. The dark grey microregion B in the metal layer is presumed to be Ti_2Cu. The grey microregion C in the metal layer is composed of Cu ss and Ti-Cu intermetallics. The light grey microregion D in the metal layer is identified as Ag ss. The EDS results of the microregions in the metal layer demonstrate that the phase components of the metal layer in the Al_2O_3/Cu joint are highly consistent with those of the metal layer in the metallized Al_2O_3. This indicates that the inter-diffusions and/or reactions between the metal layer and liquid solder can be considered to be negligible during the low-temperature joining of the metallized Al_2O_3 to Cu using Sn-Ag-Cu solder.

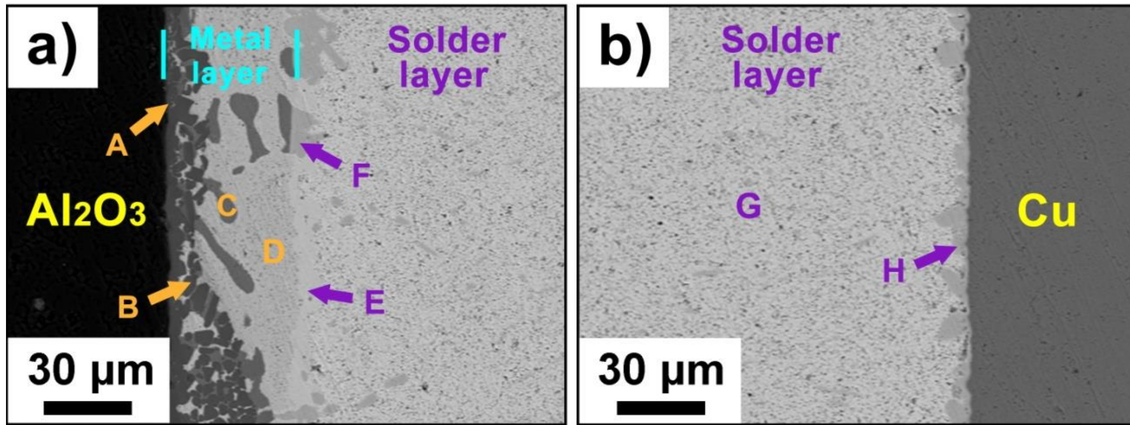

Fig. 8. Enlarged images of the interfacial region of Al_2O_3/Cu joint using Sn-Ag-Cu solder.

a) Al_2O_3/metal layer/solder layer part; b) solder layer/Cu base material part.

Table 3. EDS results of the microregions in Fig. 8.

Microregion	Compositions (at.%)						Possible phases
	Ag	Cu	Ti	Sn	Al	O	
A	0.23	15.48	36.82	-	4.62	42.85	Cu_3Ti_3O
B	0.66	34.75	64.59	-	-	-	Ti_2Cu
C	3.53	57.21	39.26	-	-	-	Cu ss, Ti_2Cu
D	95.78	3.60	0.62	-	-	-	Ag ss
E	76.64	0.13	0.00	23.23	-	-	Ag_3Sn
F	0.54	38.63	1.21	59.62	-	-	Sn ss, Cu_6Sn_5
G	1.48	0.00	-	98.52	-	-	Sn ss
H	0.61	49.33	-	50.06	-	-	Cu_6Sn_5

In the case of microregion E in the solder layer in close proximity to the metal layer,

the atomic ratio of Ag and Sn is approximately 3:1, which indicates the formation of Ag_3Sn in the light-grey region of the solder layer. In their investigation into the wettability of Sn-Ag-Cu solder on a Cu base material, Yu et al. [24] identified the presence of Ag_3Sn in the solder layer. It can be postulated that the light-grey microregion F adjacent to the metal layer is a mixture of Sn ss and Cu_6Sn_5. The grey microregion G in the solder layer exhibits a high Sn content of 98.52 at.%, indicative of Sn ss. Furthermore, the light grey microregion H in the solder layer near the Cu base material displays a Cu:Sn ratio of about 6:5, indicative of the formation of Cu_6Sn_5. In a separate study, Kim et al. [25] demonstrated that Cu_6Sn_5 could be formed in the Sn-Ag-Cu alloy.

Fig. 9 depicts the XRD pattern of the joining area of the Al_2O_3 /Cu joint utilizing Sn-Ag-Cu solder. The XRD analysis indicates the presence of various phases, including Sn, Ag, Cu, Ti_2Cu, Ag_3Sn and Cu_6Sn_5, within the joining area. The EDS results reveal that the metal layer in the joint comprises Ag ss, Cu ss and Ti_2Cu, whereas the solder layer contains Sn ss, Ag_3Sn and Cu_6Sn_5. Consequently, the diffraction peaks of Ag, Cu and Ti_2Cu in the XRD pattern may be attributed to the metal layer, while the peaks of Sn, Ag_3Sn and Cu_6Sn_5 may be indicative of the solder layer.

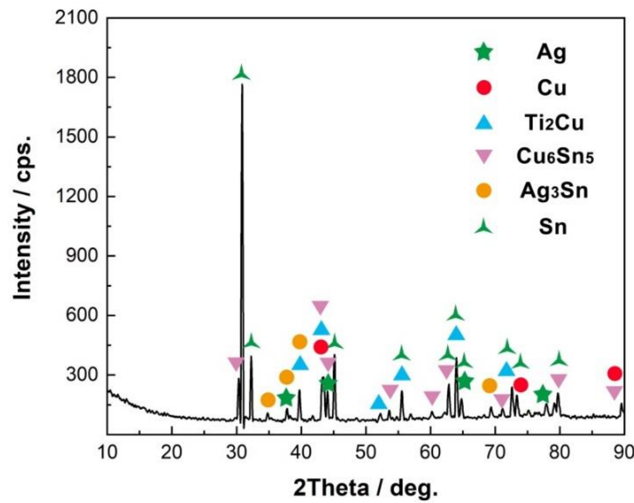

Fig. 9. XRD pattern of the joint area of Al_2O_3/Cu joint using Sn-Ag-Cu solder.

3.4 Mechanical properties of Al_2O_3/Cu joint

Fig. 10 illustrates the microhardness of the Al_2O_3/Cu joint using Sn-Ag-Cu solder. It is noteworthy that the microhardness of the Cu_3Ti_3O reaction layer was not reported due to the limited thickness (only 2~5 μm). As shown in Fig. 10, the microhardness values of the Al_2O_3 are notably high, while those of the other areas of the joint are comparatively low.

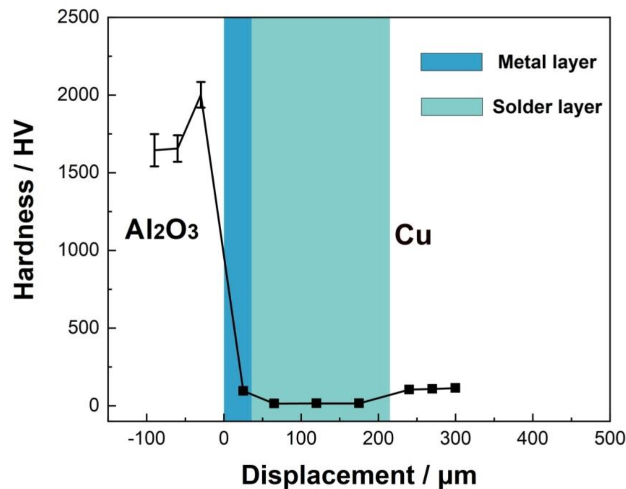

Fig. 10. Microhardness distribution in the Al_2O_3/Cu joint.

The microhardness of the Al_2O_3 in the joint exhibits regional variations. The hardness in the region remote from the joining region is 1768 ± 196 HV. Kar et al. [26] reported a comparable microhardness of the Al_2O_3 (about 1900 HV) in the Al_2O_3/304 stainless steel joint using Ag-Cu-Ti filler. However, the microhardness of Al_2O_3 in the region in close proximity to the joining region increases to 2031 ± 55 HV, which may be due to the residual stress concentration resulting from the thermal mismatch between the Al_2O_3 and Ag-Cu-Ti filler (Al_2O_3: 7.0~8.3 × 10^{-6}/°C [27]; Ag-Cu-Ti: 19.0 × 10^{-6}/°C [28]). As illustrated by Carlsson and Larsson [29], there was a positive correlation between microhardness and residual stress. Therefore, the microhardness of the Al_2O_3 in the region close to the joining region is observed to be higher than that of the Al_2O_3 in regions further from the joining region. Jin et al. [9] similarly observed that the microhardness of the Al_2O_3 in the vicinity of the joining region was greater than that of the Al_2O_3 distant from the joining region in the Al_2O_3/Cu joint brazed with Ag-Cu-Ti filler and refractory metal foil. The observed increase in hardness was attributed to the generation of significant residual stress due to the thermal mismatch in the joint.

The microhardness of the metal layer in the Al_2O_3/Cu joint is 96 ± 7 HV, which is comparable to that of Ag-Cu-Ti filler layer (107 ± 6 HV) as reported by Kang et al. [30] in carbon/carbon and Ti-6Al-4V joining with Ag-Cu-Ti and Nb foils. The solder layer in the joint exhibits a microhardness of 15 ± 2 HV, similar to that reported by Fouzder et al. [31] for Cu/Cu joining using Sn-Ag-Cu solder (15 HV). The microhardness of the Cu

base metal in the joint is 106 ± 2 HV, close to that of Cu (94 HV) as reported by Chang et al. [32].

The shear strength of the Al_2O_3/Cu joint is 21.3 ± 3.1 MPa, which is comparable to that reported by Jin et al. [9] for the Al_2O_3/Cu joint brazed with Ag-Cu-Ti filler at 900°C (24.9 MPa). **Fig. 11** presents the fracture analysis of the Al_2O_3/Cu joint following the shearing test. The fracture is located in the joining region, as illustrated in Fig. 11a). In order to clarify the precise location of the fracture, the fracture was characterized by FESEM and EDS.

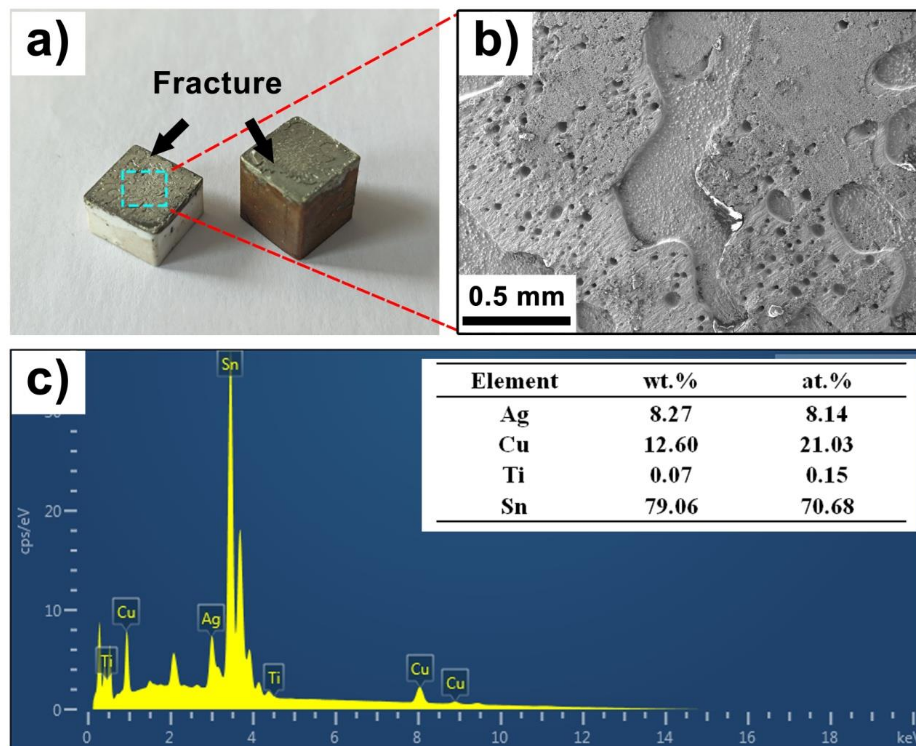

Element	wt.%	at.%
Ag	8.27	8.14
Cu	12.60	21.03
Ti	0.07	0.15
Sn	79.06	70.68

Fig. 11. Fracture analysis of Al_2O_3/Cu joint after shearing test.

a) fracture image, b) micro-morphology of the fracture area (containing the Al_2O_3 ceramics parent material part), c) EDS result of the fracture in b).

The FESEM image of the fracture (**Fig. 11b**) demonstrates the existence of a considerable number of tough fossae, indicating a ductile fracture. In addition, an irregular band structure can be observed in the fracture, which may be caused by the collision of the slip bands within the metal with the dendrites during the shearing test. The EDS analysis of the fracture region reveals the presence of elements including Sn, Ag, Cu and Ti. The concentration of Sn is relatively high (70.68 at.%), while the levels of Ag, Cu and Ti are comparatively low. The microstructure analysis of the joint reveals that the solder layer primarily contains Sn, along with a small amount of Ag and Cu, while the metal layer contains Ag, Cu and Ti. Accordingly, the EDS analysis of the fracture indicates that the fracture of the Al_2O_3/Cu joint is located in the solder layer instead of the metal layer. Fu et al. [10] illustrated that the fracture of the Al_2O_3/Cu joint brazed with Sn-Ag-Cu solder occurred within the solder layer, which is in accordance with the findings of this study. The fracture analysis of the joint demonstrates that favorable interfacial bonding can be achieved among the Al_2O_3, metal layer, solder layer and Cu base metal in metallized Al_2O_3/Cu low-temperature joining using Sn-Ag-Cu solder. The relatively low strength of Sn-Ag-Cu solder may result in relatively low shear strength of the joint. However, the interfacial bonding among the metallized Al_2O_3, the solder layer and the Cu base metal is satisfactory.

4. Conclusions

1) Surface metallization of Al_2O_3 can be achieved using Ag-Cu-Ti active metal filler at a

temperature of 900°C for a period of 10 minutes. The microanalysis indicates that the interfacial reaction occurs between the active metal filler and the Al_2O_3, resulting in the formation of a Cu_3Ti_3O reaction layer. The metal layer on the surface of Al_2O_3 mainly consisted of Ag ss, Cu ss and Ti_2Cu.

2) The microscopic analysis of the surface metal layer in the metallized Al_2O_3 shows that the oxide content can be significantly reduced after polishing treatment, which is beneficial for the subsequent low-temperature joining of the metallized Al_2O_3 to Cu.

3) Low-temperature joining of the metallized Al_2O_3 to Cu is achieved using Sn-Ag-Cu solder at 280°C. The joining area of the joint includes the Cu_3Ti_3O reaction layer, the metal layer and the solder layer. The solder layer is primarily composed of Sn ss, Ag_3Sn and Cu_6Sn_5.

4) The shear strength of the Al_2O_3/Cu joint is 21.3 ± 3.1 MPa. The Al_2O_3/Cu joint fractures in the solder layer after shearing test, indicating that the strength of the solder is relatively low. However, the interfacial bonding among the metallized Al_2O_3, the solder layer and the Cu base metal is satisfactory.

Acknowledgements

This work was supported by the WIT Graduate Education Innovation Fund (Grant No. CX2021164).

Conflicts of interest

The authors have no conflicts of interest to declare.

References

[1] W. Fu, S.P. Hu, X.G. Song, C. Jin, J.X. Li, Y.X. Zhao, J. Cao, G.D, Wang, Effect of Ti content on the metallization layer and copper/alumina brazed joint, Ceram. Int. 43 (2017) 13206-13213. https://doi.org/10.1016/j.ceramint.2017.07.016.

[2] Y.F. Jiang, X.F. Zhang, S.N. He, P.P. Lin, D.C. Wang, W. Lu, W.H. Wang, Study on brazing sealing and wave transmittance of single crystal Al_2O_3 microwave window, Heliyon 10 (2024) e25290. https://doi.org/10.1016/j.heliyon.2024.e25290.

[3] S.H. Rajendran, S.J. Hwang, J.P. Jung, Active brazing of alumina and copper with multicomponent Ag-Cu-Sn-Zr-Ti filler, Metals 11 (2021) 509. https://doi.org/10.3390/met11030509.

[4] H.J. Ji, H. Chen, M.Y, Li, Overwhelming reaction enhanced by ultrasonics during brazing of alumina to copper in air by Zn-14Al hypereutectic filler, Ultrason. Sonochem. 35 (2017) 61-71. https://doi.org/10.1016/j.ultsonch.2016.09.003.

[5] H.Y. Chen, X.W. Ren, W. Guo, M.L. Wan, Z.K. Shen, X.C. Liu, M.Y. Feng, Microstructures and mechanical properties of brazed Al_2O_3/Cu joints with bismuth glass, Ceram. Int. 45 (2019) 16070-16077. https://doi.org/10.1016/j.ceramint.2019.05.123.

[6] B.T. Li, B. Liu, Y. Wang, R.Q. Hu, Y. Wang, Z.W. Yang, Microstructure and mechanical properties of Al_2O_3 ceramic and copper joints brazed with AgCuInTi brazing alloy, Int. J. Appl. Ceram. Technol. (2024) in press. https://doi.org/10.1111/ijac.14828.

[7] L.L. Yuan, W. Wang, X.M. Huang, Y.F. Qi, X.Y. Li, Joining of Al_2O_3 to Cu with

Cu-Sn-Ti active brazing filler alloy, Weld. World. 66 (2022) 1471-1479. https://doi.org/10.1007/s40194-022-01305-5.

[8] B.B. Fan, J.K. Xu, H.C. Lei, L. Zhao, D. An, Z.P. Xie, Microstructure and mechanical properties of Al_2O_3/Cu joints brazed with Ag–Cu–Ti + Zn composite fillers, Ceram. Int. 48 (2022) 18551-18557. https://doi.org/10.1016/j.ceramint.2022.03.125.

[9] B.X. Jin, M.Q. Zou, Y.J. Zhao, S.G. Wang, Y.W. Mao, Joining of Al_2O_3 ceramic to Cu using refractory metal foil, Ceram. Int. 48 (2022) 3455-3463. https://doi.org/10.1016/j.ceramint.2021.10.123.

[10] W. Fu, X.G. Song, S.P. Hu, J.H. Chai, J.C. Feng, G.D. Wang, Brazing copper and alumina metallized with Ti-containing Sn0.3Ag0.7Cu metal powder, Mater. Des. 87 (2015) 579-585. https://doi.org/10.1016/j.matdes.2015.08.081

[11] H. Jouhara, A. Chauhan, T. Nannou, S. Almahmoud, B. Delpech, L.C. Wrobel, Heat pipe based systems-Advances and applications, Energy 128 (2017) 729-754. https://doi.org/10.1016/j.energy.2017.04.028.

[12] M. Ali, K.M. Knowles, P.M. Mallinson, J.A. Fernie, Microstructural evolution and characterisation of interfacial phases in Al_2O_3/Ag–Cu–Ti/Al_2O_3 braze joints, Acta Mater. 96 (2015) 143-158. https://doi.org/10.1016/j.actamat.2015.05.048.

[13] T. Li, H.T. Xue, X.M. Meng, W.B. Guo, S. Zhang, H. Wu, Releasing the residual stress of Al_2O_3/304 stainless steel joint by introducing BN into Ag-Cu-Ti filler metal, Int. J. Appl. Ceram. Technol. 21 (2024) 2235-2245. https://doi.org/10.1111/ijac.14607.

[14] Y. Wen, S.T. Zhang, W.Q. Huang, D.K. Yu, L. Hu, P. Wang, R.T. Fang, P.X. Ouyang, Effect of Ti content on microstructure and properties of

Cu/AgCuTi/Al_2O_3 brazed joints, Mater. Today Commun. 40 (2024) 109507. https://doi.org/10.1016/j.mtcomm.2024.109507

[15] H. Saleh, T. Weling, J. Seidel, M. Schmidtchen, R. Kawalla, F.O.R.L. Mertens, H.P. Vogt, An XPS study of native oxide and isothermal oxidation kinetics at 300 C of AZ31 twin roll cast magnesium alloy, Oxid. Met. 81 (2014) 529-548. https://link.springer.com/article/10.1007/s11085-013-9466-z.

[16] L.L. Wang, H.M. Xu, Y.X. Qiu, X.S. Liu, W.J. Huang, N.Q. Yan, Z. Qu, Utilization of Ag nanoparticles anchored in covalent organic frameworks for mercury removal from acidic waste water, J. Hazard. Mater. 389 (2020) 121824. https://doi.org/10.1016/j.jhazmat.2019.121824.

[17] T.E. Graedel, Corrosion mechanisms for silver exposed to the atmosphere, J. Electrochem. Soc. 139 (1992) 1963. https://iopscience.iop.org/article/10.1149/1.2221162.

[18] A.R. Zainun, S. Tomoya, U.M. Noor, M. Rusop, I. Masaya, New approach for generating Cu_2O/TiO_2 composite films for solar cell application, Mater. Lett. 66 (2012) 254-256. https://doi.org/10.1016/j.matlet.2011.08.032.

[19] Ç. Oruç, A Altındal, Structural and dielectric properties of CuO nanoparticles, Ceram. Int. 43 (2017) 10708-10714. https://doi.org/10.1016/j.ceramint.2017.05.006.

[20] T.W. Wu, H.T. Zhao, X.J. Zhu, Z. Xing, Q. Liu, T. Liu, S.Y, Gao, S.Y. Lu, G. Chen, A.M, Asiri, Y.N. Zhang, X.P. Sun, Identifying the origin of Ti^{3+} activity toward enhanced electrocatalytic N_2 reduction over TiO_2 nanoparticles modulated by mixed-valent copper, Adv. Mater. 32 (2020) 2000299. https://doi.org/10.1002/adma.202000299.

[21] T.W. Wu, X.J. Zhu, Z. Xing, S.Y. Mou, C.B, Li, Y.X. Qian, Q. Liu, Y.L. Luo, X.F. Shi, Y.N, Zhang, X.P. Sun, Greatly improving electrochemical N_2 reduction over TiO_2 nanoparticles by iron doping. Angew. Chem., Int. Ed. 58 (2019) 18449-18453. https://doi.org/10.1002/anie.201911153.

[22] K. Ma, R Zhang, J L Sun, C.X. Liu, Oxidation mechanism of biomedical titanium alloy surface and experiment, Int. J. Corros. 2020 (2020) 1678615. https://doi.org/10.1155/2020/1678615.

[23] G. Izuta, T. Tanabe, K. Suganuma, Dissolution of copper on Sn-Ag-Cu system lead free solder, Soldering Surf. Mount Technol. 19 (2007) 4-11. https://doi.org/10.1108/09540910810836484.

[24] D.Q. Yu, L. Wang, C.M.L. Wu, C.M.T. Law, The formation of nano-Ag_3Sn particles on the intermetallic compounds during wetting reaction, J. Alloys Compd. 389 (2005) 153-158. https://doi.org/10.1016/j.jallcom.2004.08.017.

[25] K.S. Kim, S.H. Huh, K. Suganuma, Effects of cooling speed on microstructure and tensile properties of Sn-Ag-Cu alloys, Mater. Sci. Eng. A. 333 (2002) 106-114. https://doi.org/10.1016/s0921-5093(01)01828-7.

[26] A. Kar, S. Mandal, K Venkateswarlu, A.K. Ray, Characterization of interface of Al_2O_3-304 stainless steel braze joint, Mater. Charact. 58 (2007) 555-562. https://doi.org/10.1016/j.matchar.2006.12.001.

[27] F. Cardarelli, Ceramic Refractories and Glasses, in: Materials Handbook, Springer Cham., Berlin, 2018, pp. 883-1012.

[28] Z.W. Yang, L.X. Zhang, W. Ren, M, Lei, J.C. Feng, Interfacial microstructure and strengthening mechanism of BN-doped metal brazed Ti/SiO_2-BN joints, J. Eur. Ceram. Soc. 33 (2013) 759-768.

https://doi.org/10.1016/j.jeurceramsoc.2012.10.017.

[29] S. Carlsson, P.L. Larsson, On the determination of residual stress and strain fields by sharp indentation testing. Part I: theoretical and numerical analysis, Acta Mater. 49 (2001) 2179-2191. https://doi.org/10.1016/S1359-6454(01)00122-7.

[30] Y.H. Kang, K.M. Feng, W.T. Zhang, Y.W. Mao, Microstructural and mechanical properties of CFC composite/Ti6Al4V joints brazed with Ag-Cu-Ti and refractory metal foils, Arch. Civ. Mech. Eng. 21 (2021) 113. https://doi.org/10.1007/s43452-021-00268-6

[31] T. Fouzder, Q.Q. Li, Y.C. Chan, D.K, Chan, Interfacial microstructure and hardness of nickel (Ni) nanoparticle-doped tin–silver–copper (Sn-Ag-Cu) solders on immersion silver (Ag)-plated copper (Cu) substrates, J. Mater. Sci. Mater. Electron. 25 (2014) 4012-4023. https://doi.org/10.1007/s10854-014-2123-8.

[32] Y.L. Chang, P. Mohanty, N. Karmarkar, M.T. Khan, Y.P. Wang, J. Wang, Microstructure and properties of Cu–Cr coatings deposited by cold spraying, Vacuum 171 (2020) 109032. https://doi.org/10.1016/j.vacuum.2019.109032.